

American Journal of Geospatial Technology (AJGT)

ISSN: 2833-8006 (ONLINE)

VOLUME 4 ISSUE 1 (2025)





Volume 4 Issue 1, Year 2025 ISSN: 2833-8006 (Online)

DOI: https://doi.org/10.54536/ajgt.v4i1.4619 https://journals.e-palli.com/home/index.php/ajgt

Urbanization and Its Ecological Impacts in Zanzibar: A Spatial-Temporal Analysis with Land Change Modeler (1995–2024)

Mohamed Khalfan Mohamed1*

Article Information

Received: February 23, 2025 Accepted: March 26, 2025 Published: April 30, 2025

Keywords

Zanzihar, Land Use Land Cover Change, Spectral Separability, Transformed Divergence, Jeffries-Matusita

ABSTRACT

This study examines the urban expansion of Zanzibar from 1995 to 2024, utilizing Landsat satellite imagery to highlight the role of remote sensing in understanding land-use changes and their socio-environmental implications. By employing change detection analysis, land cover classification techniques, and spectral separability assessments, the research quantifies the spatial and temporal dynamics of urban growth. Spectral separability was evaluated using Transformed Divergence (TD) and Jeffries-Matusita (J-M) distance metrics to ensure reliable differentiation between land cover classes, enhancing classification accuracy. The analysis focused particularly on urban Unguja Island and its surroundings, where significant urban sprawl has occurred over the past three decades. Results indicate a dramatic increase in built-up areas, rising from 2,650.5 ha in 1995 to 11,407.2 ha in 2024, corresponding to an overall growth of 330.4%. This urban expansion has come at the expense of natural vegetation, which decreased by 26.3% over the study period. While water bodies have remained relatively stable, the transformation of vegetation into urban land highlights the growing environmental pressure exerted by rapid urbanization. The classification accuracy of the study improved over time, with overall accuracies of 78.33%, 87.22%, and 93.33% for the years 1995, 2009, and 2024, respectively. The findings emphasize the importance of implementing sustainable urban planning and policy interventions to mitigate the adverse effects of urban sprawl on ecological sustainability. Integrating remote sensing data with socio-economic analysis is recommended for developing effective land management strategies in Zanzibar.

INTRODUCTION

Urban growth is a predominant global trend driven by economic opportunity, demographic shifts, and ruralto-urban migration. The United Nations projects that by 2050, nearly 68% of the global population will reside in urban areas, with most of this growth concentrated in Asia and Africa, where urban populations are rising rapidly (UN, 2019). Urban expansion is particularly intense in megacities like Mumbai, Lagos, and Dhaka, where populations are expected to double within the next few decades due to high migration rates and natural population increase (World Bank, 2021). As cities grow, they consume significant land resources; in developing regions, urban sprawl is encroaching on agricultural and forested areas, threatening food security and local ecosystems (Seto et al., 2020). This expansion is transforming landscapes worldwide, contributing to environmental challenges like habitat fragmentation and biodiversity loss, as well as increasing the demand for housing, infrastructure, and basic services (Angel et al., 2021). These trends underscore the complex challenges governments face in managing urban growth sustainably, ensuring cities remain livable, resilient, and equitable spaces (UN-Habitat, 2020).

The environmental impacts of global urban growth are substantial, with urban areas accounting for over 70% of global greenhouse gas emissions, despite covering only 3% of Earth's surface (UN-Habitat, 2020). Urbanization often leads to the phenomenon of urban heat islands, where built-up areas experience higher temperatures than

surrounding rural regions due to reduced vegetation and increased energy use, particularly in large cities like Tokyo and New York (Li et al., 2021). Additionally, expanding urban areas place immense pressure on water resources, as cities draw on local and regional supplies to meet the demands of growing populations (Zhang et al., 2021). Addressing these impacts requires integrated planning that includes green infrastructure, energy-efficient buildings, and compact city designs to reduce resource consumption and mitigate environmental degradation (Satterthwaite et al., 2020). Cities that have successfully implemented sustainable urban planning, such as Singapore and Stockholm, illustrate how innovative policies can manage urban growth's environmental impacts while enhancing residents' quality of life and fostering economic resilience (Sassen, 2021).

Remote sensing, particularly through the Landsat mission, has revolutionized the mapping of urban growth globally by providing comprehensive, long-term datasets that facilitate the monitoring and analysis of land-use changes. Since its launch in 1972, the Landsat program has consistently delivered high-quality satellite imagery, capturing detailed information on urban environments and their expansion (U.S. Geological Survey, 2021). One of the significant advantages of Landsat is its moderate spatial resolution of 30 meters, which enables the identification of various land cover types, including built-up areas, vegetation, and water bodies. This capability is crucial for urban studies, as it allows researchers to assess impervious surface expansion, evaluate urban heat islands,

¹ Abdulrahman Al-Sumait University, Zanzibar, Tanzania.

^{*} Corresponding author's e-mail: mohamed.khalfan76@gmail.com



and monitor the effects of urbanization on surrounding ecosystems (Seto et al., 2012). The temporal resolution of Landsat, with images acquired approximately every 16 days, provides insights into rapid urbanization dynamics, particularly in developing regions experiencing population influx and infrastructural pressures (Zhang et al., 2021). By employing advanced analytical techniques, such as change detection and classification algorithms, researchers can effectively quantify urban growth and its impacts on the environment, informing sustainable urban planning and management strategies (Tsurusaki & Salem, 2024). Landsat's extensive historical archive allows for long-term studies of urbanization trends, revealing critical insights into how cities evolve over time and the associated socio-environmental consequences (Valero-Jorge et al., 2024). For instance, studies have shown that urban expansion often encroaches on agricultural and natural landscapes, leading to habitat loss and increased vulnerability to climate change (Sánchez-Llull et al., 2025). This highlights the necessity of integrating remote sensing data into urban development frameworks to ensure balanced growth that considers environmental sustainability. Furthermore, the versatility of Landsat imagery enables its integration with other remote sensing platforms and ground-based data, enhancing the accuracy of urban growth assessments and supporting evidencebased decision-making for sustainable urban futures (Tew et al., 2018; Chander et al., 2009).

Urban growth in Zanzibar, Tanzania, reflects broader national trends of increasing urbanization driven by rapid population growth, tourism, and rural-to-urban migration (World Bank, 2021). Zanzibar is the most urbanized region in Tanzania, and its population is expanding at a rate of approximately 4.4% annually, surpassing the mainland average and creating significant demand for housing, infrastructure, and services (NBS Tanzania, 2020). The growth of the tourism sector has spurred economic development and job creation, drawing more residents to urban centers like Stone Town; however, it has also led to land-use changes that encroach on coastal ecosystems, including critical mangrove forests (RGoZ, 2020; RGoZ, 2022). With limited space for urban expansion on the island, rapid population growth contributes to overcrowding, water shortages, and inadequate waste management systems, particularly in low-income neighborhoods (UN-Habitat, 2021). Moreover, the urban infrastructure in Zanzibar is struggling to keep pace with demand, leading to challenges such as traffic congestion, insufficient public transport, and high levels of air and water pollution (RGoZ, 2022World Bank, 2021). In response, the Revolutionary Government of Zanzibar has launched the Zanzibar Urban Development Policy, aiming to promote sustainable urban growth through policies that improve infrastructure, support economic diversification, and enhance environmental resilience (RGoZ, 2020; RGoZ, 2019). However, the success of these efforts relies heavily on sustainable land use planning and greater investment in environmental conservation to

mitigate the pressures of urbanization on both natural resources and community welfare (RGoZ, 2022; World Bank, 2021).

While research on Zanzibar's urban growth has expanded, a critical research gap exists in utilizing spatial time series data to comprehensively map and analyze long-term urban expansion and its ecological impacts. Previous studies have primarily relied on general population metrics and localized surveys, which are limited in capturing the spatial and temporal patterns of landuse change over extended periods (World Bank, 2021). However, Landsat missions, with their extensive historical record spanning nearly five decades, offer a unique and valuable dataset for examining urban growth dynamics over time. The application of Land Changer Modeler in TerrSet liberaGIS v20.01 provides a robust framework for detecting gradual land conversion and encroachment on existing ecosystems and agricultural land through advanced analytical techniques such as change detection. Existing studies have overlooked the integration of spatial-temporal analysis essential for understanding the progression of urbanization over decades. Therefore, this study aims to bridge this gap by mapping Zanzibar's urban expansion from 1995 to 2025 using Landsat missions and advanced change detection techniques to provide a comprehensive understanding of urban growth patterns and their implications for ecological sustainability.

MATERIALS AND METHODS Study Area

The study area for this research is the urban region of Unguja, the largest and most populous island of the Zanzibar Archipelago, located off the coast of mainland Tanzania in East Africa (Figure 1). Unguja is situated between latitudes approximately 5.7°S and 6.5°S, and longitudes 39.0°E and 39.6°E. The island covers an area of around 1,666 square kilometers, with Zanzibar City, its capital, located on the central-western coast. The city comprises two main parts: Stone Town, a historic urban area designated as a UNESCO World Heritage Site, and Ng'ambo, a rapidly growing urban area that has undergone significant expansion over the past few decades. Zanzibar experiences a tropical monsoon climate characterized by two distinct rainy seasons: the long rains (Masika) from March to May, and the short rains (Vuli) from October to December (Mohamed et al., 2023a). The average annual temperature ranges from 25°C to 30°C, with high humidity levels due to its coastal location. Zanzibar City serves as the political, economic, and cultural hub of Zanzibar (Mohamed et al., 2023b). It has witnessed rapid population growth due to rural-to-urban migration and natural population increase. The city's economy largely relies on tourism, fishing, trade, and small-scale industries. The growth of tourism has particularly driven urban development, especially in coastal areas and transport infrastructure (Mohamed et al., 2024). The urban landscape of Zanzibar City has transformed significantly over the study period,



with increasing built-up areas replacing vegetation and agricultural land (Mohamed *et al.*, 2024). Key drivers of urbanization include population growth, tourism

development, and infrastructure expansion (Mohamed et al., 2023; Mohamed et al., 2024).

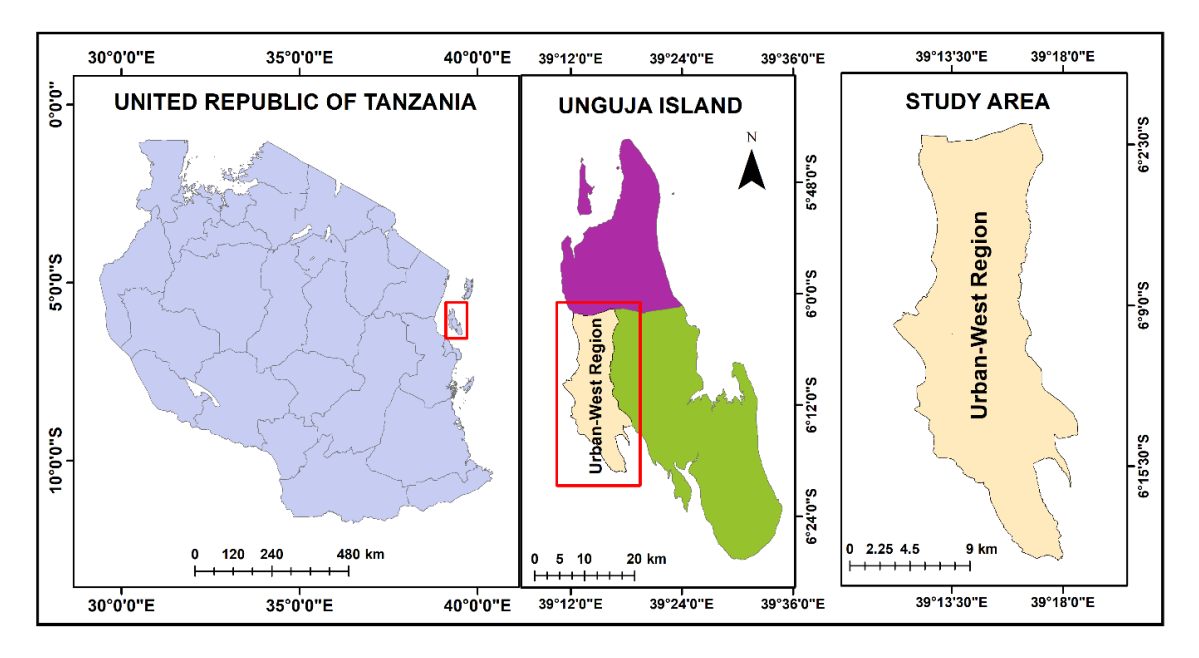


Figure 1: Study area

Data sources and pre-processing

The study utilized satellite imagery to monitor urban changes in Zanzibar from 1995 to 2024. Landsat images for the years 1995, 2009, and 2024 were acquired from the US Geological Survey's Earth Explorer portal (http://earthexplorer.usgs.gov/, last accessed 21 December 2024) to evaluate temporal shifts in urban land cover. Given Zanzibar's persistent cloud cover throughout the year, selecting suitable imagery presented a considerable challenge. However, the use of Landsat Thematic Mapper (TM), Enhanced Thematic Mapper Plus (ETM+), and Landsat 8 provided higher-resolution

data critical for accurate analysis. Landsat TM and ETM+ sensors each consist of seven spectral bands with a spatial resolution of 30 meters for most bands, while their thermal bands (band 6) have resolutions of 120 and 60 meters, respectively. Landsat 8 offers nine spectral bands with a 30-meter resolution for most bands and includes a 15-meter panchromatic band, enhancing spatial detail for improved analysis. The uneven acquisition intervals of Landsat images resulted from the region's tropical climate, characterized by frequent cloud cover and rainfall, which significantly constrained the availability of clear-sky imagery.

Table 1: The Landsat data used in the study of Zanzibar urban growth.

S/	Satellite	Bands	Acquisitio	on	WRS	Sensor	Cloud	LULC	UTM	Spatial
No.	Name	Used	Date	Time	Path/	Type	Cover	Name	Zone	Resolution
					Row		(%)			(Meters)
1	Landsat 5	1-5, 7	1995-09- 06	02.25.15	166/64	TM	1.2	1995 LULC	30 N	30 X30
2	Landsat 7	1-5, 7	2009-07- 01	02.38.27	166/64	ETM+	1.5	2009 LULC	30 N	30 X 30
3	Landsat 8	01-Jul	2024-04- 29	02.49,14	166/64	OLI	0	2024 LULC	30 N	30 X 30

The Landsat module in TerrSet liberaGIS v20.01 was employed to enhance the quality of the Landsat images through radiometric correction, converting raw digital number (DN) values into surface reflectance. To minimize atmospheric interference, the dark-object subtraction algorithm was applied, effectively reducing atmospheric haze effects. All images were reprojected to the UTM Zone 30 North coordinate system to ensure spatial

consistency across datasets. Furthermore, the Landsat images were resampled to a 15-meter spatial resolution using the nearest neighbor resampling technique, as recommended by Mota et al. (2022) and Aziz et al. (2015). This resampling process enhanced the spatial detail, enabling a more accurate analysis of urban growth patterns in Zanzibar.



Acquisition of field data

Ground control points were collected using an eTrex® 20 GPS Receiver (Garmin, Olathe, KS, USA) in combination with Landsat OLI imagery, topographic maps, and aerial photographs from the study site. These ground truth data points were acquired in February 2024. To enhance detail and improve color differentiation, a false-color Landsat OLI composite (RGB—754) was applied. Transect lines were strategically established across the study areas to capture representative samples of homogeneous land cover classes, including built-up areas, vegetation, and water bodies. For each land cover class, 60 coordinates were recorded with a precision range of 3 to 5 meters. These coordinates were then mapped onto the resampled Landsat images and converted into polygons using TerrSet Geospatial Monitoring and Modeling System (TGMMS) v20.01 by tracing the borders of the corresponding pixels. These polygons served as reference data, effectively establishing regions of interest (ROIs) that accurately represented various land cover types. The ground truth data collection followed a comprehensive approach that integrated aerial imagery and historical records. Aerial surveys, including drone imagery, provided extensive coverage and a detailed perspective of urban land cover. Additionally, archival records, such as land use maps and photographs obtained from the Zanzibar Department of Forestry, were invaluable for reconstructing longterm urban expansion trends. A thorough review of scientific literature and government reports further contextualized the findings, establishing a solid baseline for understanding urban dynamics over time.

Pre-Processing of Satellite Images

Using TerrSet Geospatial Monitoring and Modeling System (TGMMS) v20.01 software, satellite images were pre-processed for different purposes including geometric radiometric calibration, atmospheric correction, and image enhancement. Geo-referencing images was used to remove geometric distortions in the acquired data and position the satellite images into a geographical coordinate system. Pre-processing satellite images is essential before image classification to monitor and predict land use/cover changes (Mishra et al., 2017). Ground control points (GCPs) were utilized along with reference datasets from high-resolution Google Earth images, topographic maps, and aerial data obtained from Zanzibar's Department of Forestry and Department of Land Surveying. The satellite images were rectified to eliminate atmospheric distortions caused by variations in sensor orientation parameters and noise from the acquisition platform (Ma et al., 2020). This correction significantly minimized data misinterpretation during image classification. Additionally, image enhancement techniques were applied to improve the visual quality and clarity of the satellite images for subsequent analysis (Foody, 2002).

Spectral separability

To evaluate the spectral separability of various land cover types, their multispectral response patterns were thoroughly analyzed. Spectral separability reflects the statistical distance between class signatures, which significantly influences overall classification accuracy (Jackson & Adam, 2021). This study utilized the Transformed Divergence (TD) index and the Jeffries-Matusita (J-M) distance as key metrics for assessing separability. Divergence (D) values were computed using the mean and variance-covariance matrices of the feature class data, following the methodology outlined by Liu et al. (2020).

$$D_{tj} = \frac{1}{2} tr \left[(\Sigma_t - \Sigma_j) (\Sigma_j^{-1} - \Sigma_t^{-1}) \right] + \frac{1}{2} tr \left[(\Sigma_t^{-1} + \Sigma_j^{-1}) (\mu_t - \mu_j) (\mu_t - \mu_j)^T \right]$$
 (1)

The Transformed Divergence (TD) metric was employed to minimize the influence of highly separable classes, which could otherwise skew the average divergence value and diminish the reliability of the measure (Kavzoglu & Mather, 2000).

$$TD_{ij} = c \left[1 - e^{\frac{-D_{ij}}{8}} \right] \tag{2}$$

In this context, $tr[\cdot]$ denotes the trace of a matrix, which is the sum of its diagonal elements. Σi and Σj represent the variance-covariance matrices corresponding to classes i and j, respectively, while μi and μj are the associated mean vectors. The constant c defines the range of TD values.

The Jeffries-Matusita (J-M) distance measures the separability between the distributions of two classes, ω i and ω j, as described by Jia *et al.* (1999).

$$JM_{ii} = 2(1-e^{-Bij})$$
 (3)

where Bij represents the Bhattacharyya distance, calculated as (Kailath, 1967):

$$B \qquad _{ij} = \frac{1}{8} \left(\mu_i - \mu_j \right)^T \left(\frac{\Sigma_i + \Sigma_j}{2} \right)^{-1} \left(\mu_i - \mu_j \right) + \frac{1}{2} ln \left(\frac{1}{2} \frac{|\Sigma_i + \Sigma_j|}{\sqrt{|\Sigma_i||\Sigma_j|}} \right) \tag{4}$$

In this context, μi and μj represent the mean reflectance values for species i and j, respectively, while Σi and Σj denote their corresponding covariance matrices. The determinants of these matrices are given by $|\Sigma i|$ and $|\Sigma j|$. The notation $|\Sigma i|$ in refers to the natural logarithm, and $|\Sigma i|$ denotes the matrix transposition operation. According to Jensen (2005), class separability is assessed based on the resulting value: values above 1.9 indicate good separability, values between 1.7 and 1.9 suggest moderate separability, and values below 1.7 imply poor or non-existent separability.

Pairwise feature comparison

A pairwise comparison technique was used to compute similarity scores for each pair of Landsat bands based on the method outlined by Li *et al.* (2016). The bands are considered co-referent if their similarity score exceeds a specified threshold. The outcomes of these comparisons are structured into a matrix that represents the ratings between the k-th and p-th criteria. This matrix exhibits



(Ckp = 1 when k = p). Table 2 presents a correlation

reciprocity $c_{pk} = c_{kp}^{-1}$ and has unity along its diagonal matrix that illustrates the relationships between the Landsat 8 bands.

Table 2: Spectral separability as calculated by TD index (Equation (2)) and J-M distance (Equation (3)); BA-built areas, V-vegetation, W-water.

	TM (1995)		ETM+ (2009)		OLI (2020)	
LULC Pairs	TD Index	J-M Distance	TD Index	J-M Distance	TD Index	J-M Distance
BA/V	1.99	1.98	2.00	2.00	2.00	2.00
BA/W	2.00	2.00	2.00	2.00	2.00	2.00
V/W	2.00	2.00	2.00	2.00	2.00	2.00

Image classification

Image classification is a widely used and effective technique for processing satellite imagery data (Abd El-Hamid et al., 2020). This method enables the detection, identification, and categorization of various features within an image based on the actual land cover classes they represent on the Earth's surface (Huang et al., 2020). The maximum likelihood classification (MLC) algorithm was applied to classify Landsat images due to its well-established theoretical framework and versatility in handling various data types, land use, and land cover (LULC) categories across different satellite systems (Foody, 2002). This study employed a supervised classification approach utilizing the Maximum Likelihood Classifier (MLC) to classify the acquired satellite imagery. The MLC, commonly known as the Bayesian decision rule, is among the most frequently applied supervised classification algorithms due to its accessibility and straightforward training process (Huang et al., 2020). In this technique, pixels within the satellite images are classified based on their likelihood of belonging to a particular land use and land cover (LULC) category. The method operates under the assumption that all classes have equal probabilities and that the input bands follow a normal distribution. The study utilized specific input bands to generate false-color composite maps. For Landsat 5 TM and Landsat 7 ETM+, bands 4, 3, and 2 were used, while for Landsat 8 OLI, bands 5, 4, and 3 were selected. The spectral signatures of individual image pixels were compared with the training samples from the study area to classify the satellite images into three major land use/land cover (LULC) categories. These categories included built-up or urban areas, vegetation, and water bodies, as outlined in Table 3. As described by (Vali et al., 2020; Valero-Jorge et al., 2024; World Bank, 2021), the algorithm used to calculate the maximum likelihood (Li) of an unknown measurement vector (x) belonging to a specific known class (Mc) is based on the application of the Bayesian equation, which is presented in Equation (1). $L_i(x) = \ln p(a_c) - [0.5 \ln(|Cov_c|)] - [0.5(X - M_c)^T]$ $(Cov_c^{-1})(X - M_c)$ (5)

The discriminant function in the maximum likelihood algorithm is represented by Li(x), where the class is denoted as ac, with i ranging from 1 to M, where M is the total number of classes. x is an n-dimensional vector representing the pixel, and n corresponds to the number of bands. p(ac) indicates the probability of class ac at position x for a given pixel. The determinant of the covariance matrix for the data in class ac is represented by | Covc |, while Covc denotes the inverse of the covariance matrix, and Mc is the mean vector for the class.

Table 3: Classification system for land use and land cover (LULC)

	,	,
S/No.	Land Use/Land Cover Types	Description
1	Bult-up/urban	Regions that encompass residential, industrial, and commercial zones,
		as well as mixed-use structures, roadways, and other transportation
		infrastructure.
2	Vegetation	It includes agricultural and horticultural lands, crop and fallow fields,
		forests, shrubs, Coconut trees, and various other types of plantations.
3	Water Bodies	These areas encompass the city's permanent bodies of water, including
		seawater, streams, ponds, and various reservoirs.

Accuracy assessment

In this research, an accuracy assessment of the classified Landsat images was performed using ArcGIS version 10.1 to evaluate the reliability and effectiveness of the classification process. The first step in the accuracy assessment involved gathering ground truth data, which consisted of field observations or high-resolution reference datasets, to serve as the standard for comparison with the classified imagery (Cohen, 1960). These reference points were carefully selected to represent a variety of

land cover types within the study area. The confusion matrix was generated by comparing the classified image with the reference data. This was done by creating a point or polygon layer that contained the reference data and then using ArcGIS tools such as "Extract Values to Points" to compare the ground truth values with the classified image results. The confusion matrix, which is typically created using the "Tabulate Area" or "Reclassify" tool, includes key metrics such as user's accuracy (UA), producer's accuracy (PA), overall accuracy, and the kappa



statistic. The user's accuracy (UA) and the producer's accuracy (PA) were calculated for each land cover class to determine the classification's performance from both the user's and the producer's perspectives (Fleiss et al., 2003). The overall accuracy, representing the percentage of correctly classified pixels, was also derived from the confusion matrix. The kappa statistic was calculated to measure the agreement between the classified data and the reference data, correcting for random chance. The kappa coefficient is a statistical measure that ranges from -1 to 1, though it typically lies between 0 and 1. It is used to evaluate the degree of agreement between observed and predicted classifications. The interpretation of kappa values is generally categorized as follows: (i) values between 0.00 and 0.20 indicate slight agreement, (ii) values from 0.21 to 0.40 represent fair agreement, (iii) values ranging from 0.41 to 0.60 correspond to moderate agreement, (iv) values from 0.61 to 0.80 reflect substantial agreement, and (v) values between 0.81 and 1.00 signify near-perfect or almost perfect agreement (Zanotta et al., 2018). These metrics were visualized and interpreted within ArcGIS to assess the classification quality and guide any necessary improvements or adjustments. The results from the accuracy assessment were used to validate the classification method and ensure the classified image accurately represented the land cover changes observed in the field (Cohen, 1960). This process provided valuable insights into the accuracy of the LULC maps and the effectiveness of the classification approach employed in the research.

Overall Accuracy (OA) =
$$\left[\frac{(PC) + (NC)}{(PC) + (FP) + (NC) + (FN)} \right]$$
 (6)

Kappa Coefficient (K) =
$$\frac{OA - P(e)}{1 - P(e)}$$
 (7)

where, OA represents the overall accuracy, which refers to the proportion of instances that are accurately classified. Pc denotes the count of positive cases correctly identified, while Nc refers to the number of negative cases accurately classified. Fp corresponds to the number of negative cases that are incorrectly labeled as positive, and Fn represents the positive cases that are mistakenly classified as negative. P(e) is the expected probability of agreement by chance, calculated as the ratio of the sum of the products of marginal probabilities for each class to the total number of entries across all classes.

Change detection analysis

This study, the Land Change Modeler (LCM) in the TerrSet Geospatial Monitoring and Modeling System (TGMMS), was utilized to perform a change detection analysis of Landsat images from 1995, 2009, and 2024 to map urban growth in Zanzibar. The primary objective was to assess the expansion of urban areas. The analysis focused on three main land cover classes: Build-up, Vegetation, and Water. The first step involved classifying the Landsat images for each period (1995, 2009, and 2024) into the three land cover classes using TerrSet's Maximum Likelihood Classification (MLC) algorithm. This method was chosen to handle the spectral variability across

different land cover types and provide a statistically sound classification (Shivakumar *et al.*, 2018). Ground truth data was used to train the classification model, ensuring that the results accurately represented the land cover types in Zanzibar. After classification, the Land Change Modeler was used to perform change detection between the three time periods. The tool generates a change matrix that compares the classified land cover maps from 1995, 2009, and 2024, allowing for the identification of changes in the land cover classes over time. This process reveals areas where Build-up areas have expanded at the expense of Vegetation or Water, and how the spatial distribution of these classes has shifted.

The Land Change Modeler's "Change Detection" module quantifies the amount of change in each land cover class by calculating the area of transition between different classes (Pontius & Cheuk, 2006). The analysis showed how Vegetation and Water were converted to Build-up areas. This allows for a clear understanding of urban expansion patterns, including the rate and direction of growth. The Land Change Modeler was also used to predict future changes based on historical trends. By analyzing the patterns of urban growth from 1995 to 2024, the tool modeled future land cover scenarios and estimated how the Build-up area may continue to expand, potentially encroaching on Vegetation in the next 50 years. The results of the change detection analysis provided a detailed view of urban growth in Zanzibar, highlighting the transformation of land cover over the past few decades.

RESULTS AND DISCUSSIONS

Spectral separability between land cover classes

The analysis of average spectral reflectance curves for the land cover/use classes in the study area revealed distinct patterns, as depicted in Figure 2. These curves, along with their standard deviations (SDs), show considerable spectral overlaps between the three LULC classes (Builtup, Vegetation, and Water) across the seven Landsat bands, especially within 1 SD. The visible bands (bands 1 to 4: coastal aerosol, blue, green, and red) exhibited the highest level of overlap. The general reflectance trend showed that the visible bands had the lowest values, followed by band 7 (Short-wave Infrared 2), band 6 (Short-wave Infrared 1), and band 5 (Near Infrared). Among these, the near-infrared band (band 5) displayed the most noticeable reflectance differences between water and non-water classes. Outside the range of 1 SD, only the Near Infrared (band 5) and Short-wave Infrared 1 (band 6) bands were effective in distinguishing water from other land cover types. These findings highlight the significance of specific spectral bands in accurately differentiating water from other land cover classes.

Table 2 presents the spectral separability assessment of four LULC classes—built-up areas, water, and vegetation—using Landsat OLI imagery (bands 1–7) and evaluated through the Transformed Divergence (TD) and Jeffries—Matusita (J-M) distance metrics. The analysis

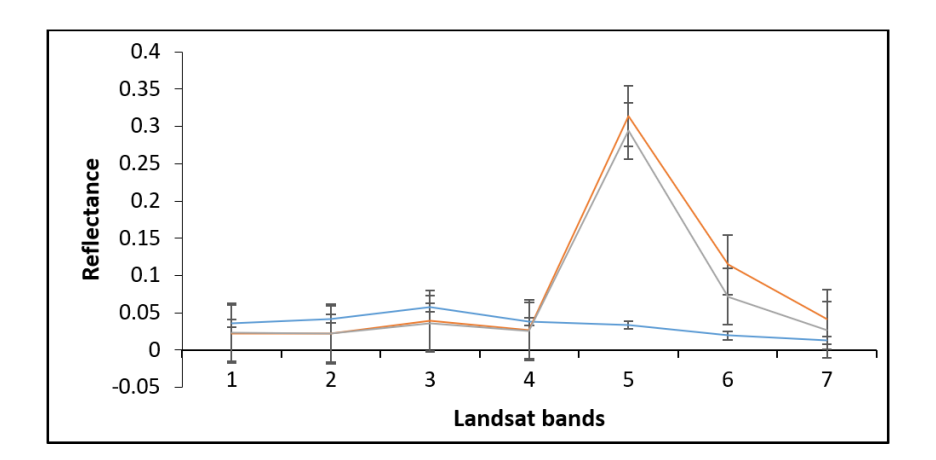


Figure 2: Mean spectral response—extracted from the Landsat OLI imagery - of land cover and land use classes in Urban Zanzibar.

showed that for Landsat OLI (2024), ETM+ (2009), and TM (1995) imagery, the TD values for all LULC classes surpassed the threshold of 1.9, indicating a clear distinction between classes. However, the assessment of Landsat TM imagery revealed limitations in differentiating certain classes: both the TD index and J-M distance demonstrated poor separability between water and built-up areas, as well as between vegetation and built-up areas. These results suggest that the older Landsat TM sensor has a reduced capacity for distinguishing specific LULC classes, highlighting the superior performance of newer sensors (ETM+, OLI) for classification tasks.

Pairwise band comparison

The pairwise correlation analysis between the Landsat bands for the urban Zanzibar scene reveals significant relationships among the spectral bands, particularly within the visible spectrum. As shown in Table 3, Bands 1 (Coastal Aerosol), 2 (Blue), 3 (Green), and 4 (Red) exhibit extremely high correlations, with values ranging from 0.979 to 0.999. This strong inter-band correlation suggests that these bands capture similar spectral information, likely due to their proximity within

the electromagnetic spectrum and their sensitivity to surface reflectance characteristics of built-up areas and vegetation. In contrast, Bands 5 (Near Infrared), 6 (Short-Wave Infrared 1), and 7 (Short-Wave Infrared 2) show moderate to high correlations with the visible bands but display a noticeable decline in correlation values, particularly with Band 5 (NIR) showing lower correlations with Bands 1-4 (0.681 to 0.783). The higher correlation between Bands 6 and 7 (0.961) reflects their shared sensitivity to moisture content and built-up surfaces, which makes them valuable for distinguishing urban areas from vegetative and water-covered regions. Furthermore, the correlation between Bands 5 and 6 is notably high (0.963), emphasizing the importance of the NIR and SWIR regions for differentiating water bodies from other land cover classes. These findings indicate that the near-infrared and Short-Wave Infrared bands offer critical information that complements the visible bands, enhancing the ability to discriminate between urban, vegetation, and water classes. The results highlight the need for careful selection of spectral bands when performing classification tasks in urban environments like Zanzibar.

Table 3: Pairwise correlations between Landsat bands for the scene covering Urban Zanzibar.

					0		
	Band 1	Band 2	Band 3	Band 4	Band 5	Band 6	Band 7
Band 1		0.999	0.980	0.994	0.681	0.790	0.902
Band 2			0.979	0.993	0.662	0.776	0.893
Band 3				0.985	0.783	0.868	0.936
Band 4					0.707	0.820	0.925
Band 5						0.963	0.869
Band 6							0.961
Band 7							

Image classification

The analysis of land cover changes in urban Zanzibar from 1995 to 2024 reveals a pronounced trend of urban expansion accompanied by a substantial decline in vegetative cover (Table 4; Figure 3). This pattern

reflects rapid urbanization driven by population growth, infrastructure development, and the expansion of settlements. Notably, built-up areas have significantly increased from 2,650.5 hectares in 1995 to 5,862.4 ha in 2009 and further to 11,407.2 ha in 2024, representing a



growth of approximately 120.9% between 1995 and 2009 and an additional 94.6% from 2009 to 2024. This rapid increase in built-up areas underscores the aggressive nature of urbanization within the study area, highlighting the urgent need for sustainable urban planning and management. Conversely, vegetation cover has been steadily declining throughout the same period, decreasing from 33,252.1 ha in 1995 to 29,801.8 ha in 2009 and subsequently to 24,496.2 ha in 2024, corresponding

to an overall reduction of approximately 26.3% from 1995 to 2024. This decline in vegetation is likely due to the conversion of natural land to built-up areas and agricultural activities to accommodate the growing population. In contrast, water bodies have exhibited minimal variation over the study period, with coverage increasing slightly from 21,773.6 ha in 1995 to 22,012.0 ha in 2009, before decreasing marginally to 21,772.8 ha in 2024.

Table 4: Land Cover Changes in Urban Zanzibar from 1995 to 2024 (in Hectares)

LULC	1995	2009	2024
	Land Cover in Hectare	es	
Built up	2,650.5	5,862.4	11,407.2
Vegetation	33,252.1	29,801.8	24,496.2
Water	21,773.6	22,012.0	21,772.8

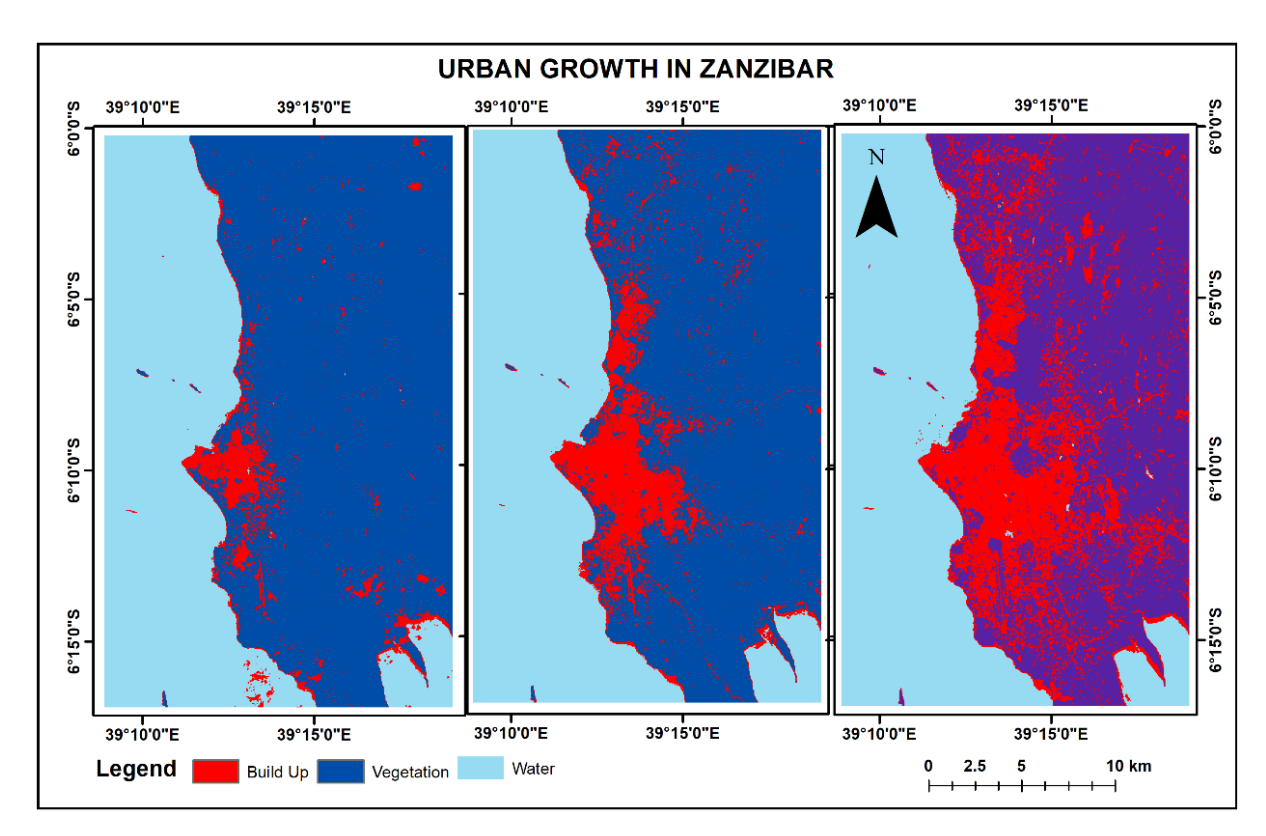


Figure 3: Zanzibar urban growth from 1995, 2009, and 2024

The analysis of land cover changes in urban Zanzibar over the periods 1995–2024 and 2009–2024 reveals a consistent trend of rapid urban expansion at the expense of vegetation cover, with minimal changes in water bodies (Figure 4). From 2009 to 2024, built-up areas experienced significant growth, with approximately 72,691 ha of land converted to urban use, while only around 11,082 ha were lost to other land covers. This net positive change underscores the aggressive urbanization occurring within the region. During the same period, vegetation exhibited a substantial net loss of approximately 69,765 ha, with only minor gains of about 10,813 ha, suggesting

limited reforestation or conservation efforts. Water bodies remained relatively stable, with a minor decrease of 3,289 ha and a small gain of 632 ha, indicating that urbanization has had minimal impact on aquatic environments thus far. However, when considering the long-term change from 1995 to 2024, the expansion of built-up areas is even more pronounced, with gains reaching approximately 90,000 ha. Vegetation loss during this period is similarly alarming, with around 70,000 ha lost and only minimal recovery. The minimal variation in water bodies between these periods suggests a degree of resilience or protection, although slight fluctuations could



indicate emerging pressures from urban growth. The overall pattern highlights the continuous and aggressive urbanization of Zanzibar, primarily driven by population

growth, infrastructure development, and settlement expansion.

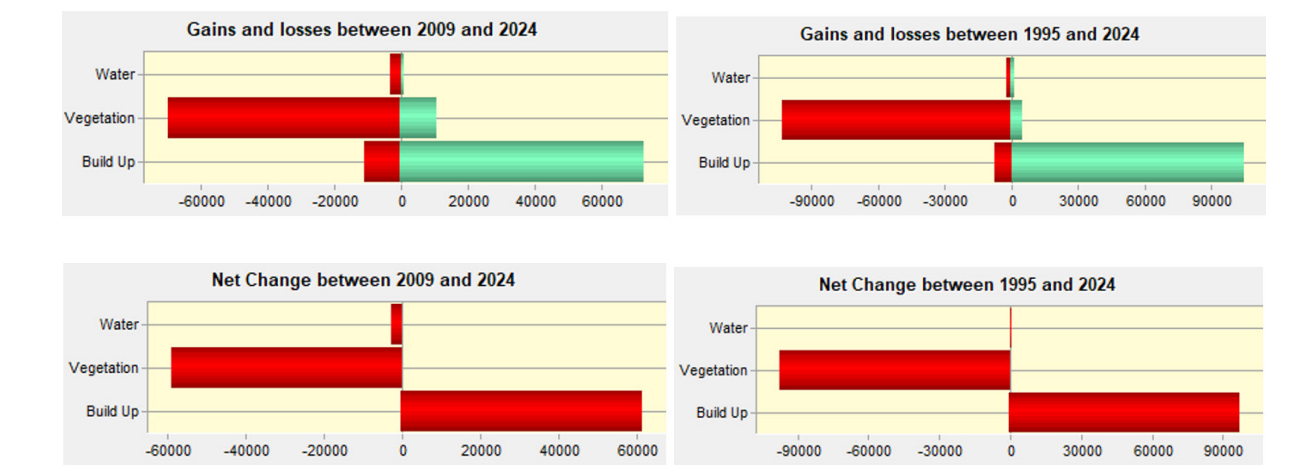


Figure 4: Land cover gain, loss, and net change from 1995 to 2024

Accuracy assessment

The accuracy assessment of the land use and land cover (LULC) classification results for urban Zanzibar demonstrates a progressive improvement in classification accuracy over the study period from 1995 to 2024. The overall accuracy and Kappa coefficient values indicate the reliability and consistency of the classification process. In 1995, the classification achieved an overall accuracy of 78.33% with a Kappa coefficient of 0.76, reflecting moderate agreement between the classified map and

ground reference data. By 2009, the accuracy significantly improved to 87.22% with a corresponding Kappa coefficient of 0.84, indicating substantial agreement. This improvement is attributed to enhanced image quality from ETM+ and OLI satellite missions and the adoption of more advanced classification techniques. In 2024, the classification accuracy reached its highest level at 93.33%, with a Kappa coefficient of 0.88, indicating a near-perfect agreement between classification results and ground reference data.

Table 5: The overall accuracies and Kappa coefficients for LULC in urban Zanzibar

Year	Ground data	Classification results	Overall accuracy (%)	Kappa coefficients
1995	180	141	78.33%	0.76
2009	180	157	87.22%	0.84
2020	180	168	93.33%	0.88

Change detection analysis

The crosstabulation analysis of 1995 and 2024 land cover maps highlights significant land cover transitions in urban Zanzibar, revealing notable urban expansion and landscape dynamics (Table 6; Figure 5). The most substantial transition is from Vegetation to Build-up, with a conversion of approximately 9,236.88 hectares, indicating extensive urbanization over the study period. This change suggests the rapid transformation of vegetated areas into urban landscapes, likely driven by population growth, infrastructure development, and economic activities. The persistence of Build-up areas (1,994.7 ha) further confirms urban growth's stability and

consolidation over nearly three decades. Additionally, the conversion from Water to Build-up (175.5 ha) illustrates the construction of houses, hotels, and infrastructure development in the coastal areas. A considerable portion of the landscape remains vegetated (23,995.3 ha), suggesting that while urban expansion is substantial, natural or semi-natural areas still dominate much of the landscape. Findings also reveal that the conversion of Build-up areas back to Vegetation (499.0 ha) is relatively minor. The minimal transition from Water to Vegetation (1.8 ha) is negligible and may reflect natural processes such as sediment deposition or slight vegetative growth along water bodies.



Table 6: Land cover transition from 1995 to 2024 in urban Zanzibar

No.	Land cover Transition	Rate of Change (in ha.)
1	Build up to Build up	1994.7
2	Vegetation to Build up	9236.8
3	Water to Build up	175.5
4	Build up to Vegetation	499.0
5	Vegetation to vegetation	23995.3
6	Water to vegetation	1.8
7	Build up to Water	156.7
8	Vegetation to Water	19.8
9	Water to water	21596.2

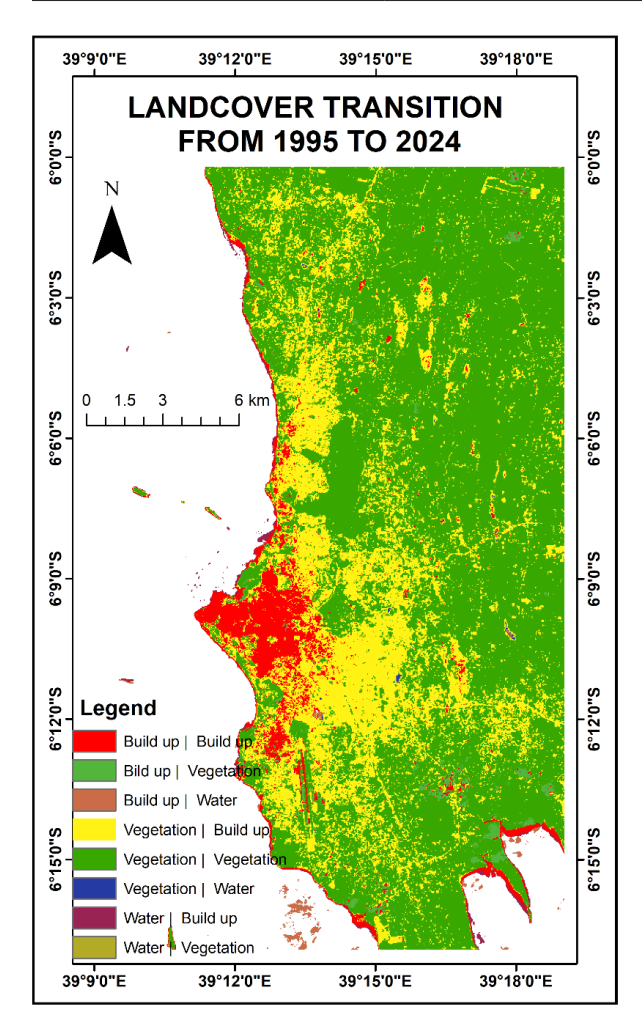


Figure 5: Land cover transitions from 1995 to 2024

The findings of land cover exchanges in urban Zanzibar between 1995 and 2024 reveal a clear pattern of extensive vegetation loss due to urban expansion, with some minor regeneration of built-up areas back to vegetation (Table 7; Figure 6). Between 1995 and 2009, 4,009.4 ha of vegetation were converted to built-up areas. This period marked the beginning of significant urbanization when natural vegetation was increasingly cleared for infrastructure development and urban growth. However, 563.8 ha of built-up land was reclaimed by vegetation, which could be attributed to greening efforts, abandonment of urban

areas, or natural vegetation regrowth. The period from 2009 to 2024 shows an even more accelerated rate of vegetation loss, with 6,251.4 ha being converted to built-up areas. During this period, 967.9 ha of built-up land was reclaimed by vegetation. The overall analysis from 1995 to 2024 indicates that a total of 9,236.8 ha of vegetation was converted to built-up areas, underscoring the significant scale of urbanization that has taken place over the past 29 years. Conversely, only 499.0 ha of built-up areas were reclaimed by vegetation throughout this period, which is relatively small compared to the vast areas lost to urbanization. The findings highlight a clear and consistent pattern of vegetation cover loss to urban expansion in urban Zanzibar, with accelerated rates of conversion occurring between 2009 and 2024.

Table 7: Exchange between vegetation and build-up areas

arcas	iicas					
Land Cover	1995-2009	2009-2024	1995-2024			
Exchange						
Land Cover Exchange	1995-2009	2009-2024	1995-2024			
Vegetation to Build Up	4009.4	6251.4	9236.8			
Build Up to Vegetation	563.8	967.9	499.0			

Discussion

Spectral separability between land cover classes

The analysis of average spectral reflectance curves for the land cover/use classes in the study area revealed distinct patterns. These curves, along with their standard deviations (SDs), show considerable spectral overlaps between the three LULC classes (Built-up, Vegetation, and Water) across the seven Landsat bands, especially within 1 SD. This observation is consistent with previous research that highlights the challenges of spectral separability between these land cover types, particularly when using multispectral sensors (Vali *et al.*, 2020). Gavade and Rajpurohit (2020) found that the visible bands (bands 1 to 4: coastal aerosol, blue, green, and red) exhibited the highest level of overlap. These findings align with studies that show the visible spectrum generally struggles to distinguish between vegetation and built-up areas due to



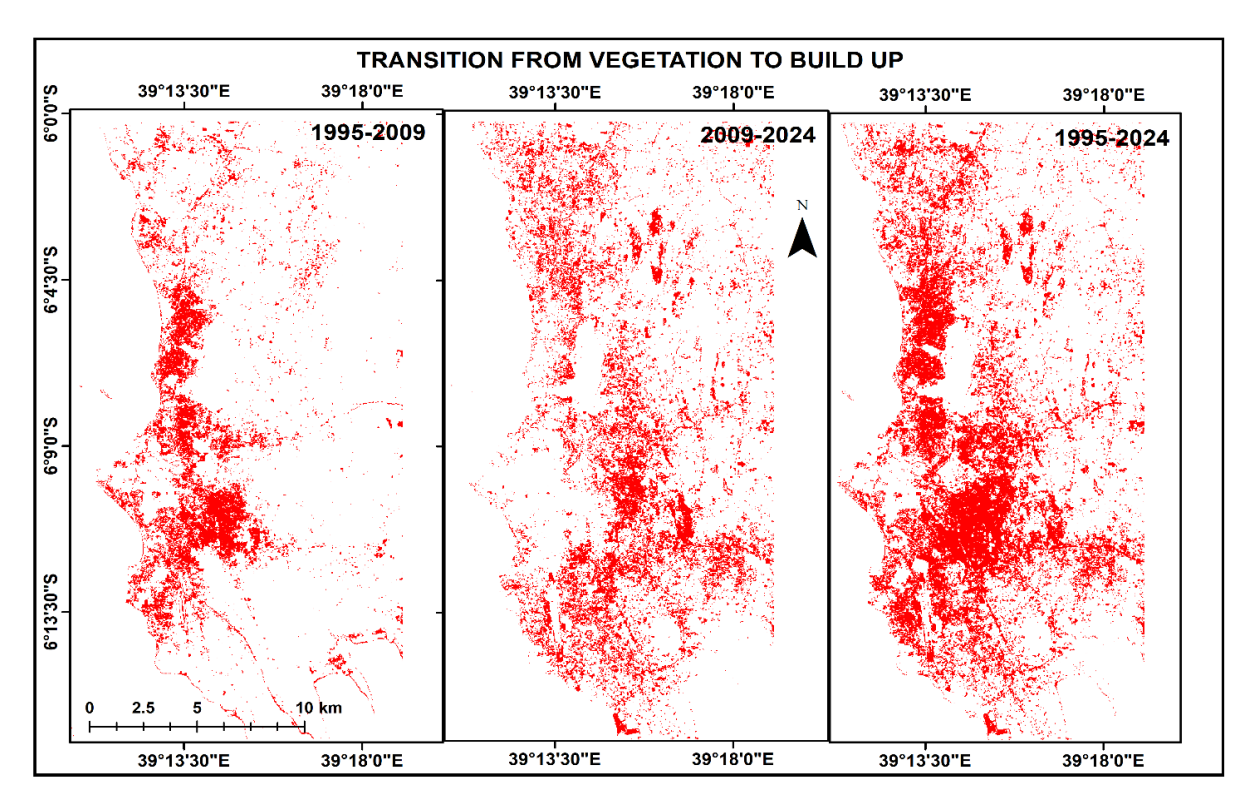


Figure 6: Transition from vegetation to build-up areas

similar reflectance characteristics in these bands (Ma et al., 2020). The general reflectance trend showed that the visible bands had the lowest values, followed by band 7 (Short-wave Infrared 2), band 6 (Short-wave Infrared 1), and band 5 (Near Infrared) (Nalepa et al., 2019). This is in agreement with other studies that have reported the effectiveness of infrared bands, particularly bands 5 and 7, in enhancing classification accuracy for land cover mapping (Gavade & Rajpurohit, 2020). Among these, the near-infrared band (band 5) displayed the most noticeable reflectance differences between water and non-water classes. This is consistent with the findings of a study by Vali et al. (2020), who demonstrated that the near-infrared region is sensitive to water body characteristics, enabling better discrimination between water and vegetation. Outside the range of 1 SD, only the Near Infrared (band 5) and Short-wave Infrared 1 (band 6) bands were effective in distinguishing water from other land cover types (Nelapa et al., 2019). Similar results were reported by Ma et al. (2020), who emphasized the significance of these bands in water body identification, especially when the spectral reflectance of water overlaps with that of vegetation in the visible bands.

The spectral separability assessment of built-up areas, water, and vegetation using Landsat OLI (2024), ETM+ (2009), and TM (1995) imagery, evaluated through Transformed Divergence (TD) and Jeffries-Matusita (J-M) distance metrics, demonstrated that newer sensors (OLI and ETM+) provide superior separability due to their enhanced spatial and spectral resolution, with TD values surpassing the 1.9 threshold for all land cover classes. This aligns with findings that newer sensors,

particularly OLI, improve classification accuracy for challenging land covers like water and urban areas (Harrak et al., 2025). In contrast, Landsat TM showed limitations in distinguishing water from built-up areas and vegetation, likely due to spectral overlap and the absence of a coastal aerosol band (Lewis et al., 2018; Günen & Atasever, 2024). These limitations are consistent with previous studies highlighting the reduced capacity of TM to separate LULC classes due to its coarser spectral resolution and fewer bands (Shao et al., 2023). Recent studies also emphasize the improved classification performance of OLI and ETM+ sensors for urban and water bodies, which are critical for accurate land cover classification and environmental monitoring (Zhang et al., 2025; Harrak et al., 2025).

Pairwise band comparison

The pairwise correlation analysis of Landsat bands for the urban Zanzibar scene revealed high correlations among visible bands (1–4), with values ranging from 0.979 to 0.999, indicating they capture similar spectral information. This is consistent with previous studies showing visible bands' effectiveness in distinguishing built-up areas and vegetation (Cottrell *et al.*, 2024). Bands 5 (NIR), 6 (SWIR 1), and 7 (SWIR 2) showed moderate correlations with visible bands, with Band 5 having lower correlations (0.681 to 0.783). The high correlation between Bands 6 and 7 (0.961) highlights their shared sensitivity to moisture content, aiding in distinguishing urban areas from vegetation and water (Gokool *et al.*, 2024). The strong correlation between Bands 5 and 6 (0.963) emphasizes the importance of NIR and SWIR





bands for differentiating water bodies (Liu et al., 2020), reinforcing the need for careful spectral band selection in urban environments like Zanzibar.

Image classification

The analysis of land cover change in urban Zanzibar from 1995 to 2024 highlights significant urban expansion, with built-up areas increasing by 120.9% from 1995 to 2009 and a further 94.6% from 2009 to 2024. This rapid urbanization, largely driven by population growth and infrastructure development, mirrors similar trends observed in coastal cities worldwide (Tsurusaki & Salem, 2024). For instance, studies in coastal cities like Lagos, Nigeria, and Jakarta, Indonesia, also report significant urban sprawl at the expense of natural ecosystems, particularly mangrove forests, and wetlands, due to high population growth and economic development (Kukkonen et al., 2017; Seto et al., 2012). Zanzibar's 26.3% loss in vegetation cover from 1995 to 2024 is consistent with the global pattern of urban encroachment into green spaces. For example, a study on urbanization in the Philippines found a comparable decline in forest cover as urban areas expanded rapidly, threatening biodiversity and ecosystem services (Tossoukpe et al., 2025). Additionally, the reduction in vegetation in Zanzibar, likely driven by land conversion for urban settlements and agriculture, mirrors findings from other African coastal cities, such as Mombasa, Kenya, where land-use changes for urbanization have led to similar declines in coastal forest and mangrove habitats (Haldar et al., 2024). On the other hand, the minimal variation observed in Zanzibar's water bodies over the study period stands in contrast to trends in cities like Dhaka, Bangladesh, where urbanization has significantly altered hydrological patterns, often leading to the reduction of freshwater bodies (Tessema & Abebe, 2023). This relative stability in Zanzibar could indicate effective conservation efforts or natural limitations in the expansion of urban development into water-rich areas, but it also suggests that Zanzibar may still face risks from future urbanization if water resource management is not carefully integrated into development plans (Barman et al., 2024). The findings from Zanzibar thus resonate with broader global challenges faced by coastal cities, reinforcing the need for sustainable urban planning that prioritizes ecological conservation, integrated ecosystem management, and climate resilience to mitigate the adverse effects of rapid urban growth (Puplampu & Boafo, 2021; Blakime et al., 2024).

Accuracy assessment

The accuracy assessment of land use and land cover (LULC) classification for urban Zanzibar shows a consistent improvement over the study period from 1995 to 2024, reflecting advancements in remote sensing technology and classification methodologies (Sánchez-Llull *et al.*, 2025). The overall accuracy increased from 78.33% in 1995, with a Kappa coefficient of 0.76 indicating moderate agreement, to 87.22% in 2009,

with a Kappa coefficient of 0.84 indicating substantial agreement. The significant improvement observed in 2009 is mainly attributed to the use of the Landsat ETM+ sensor, which offered better spectral resolution and data quality than the older Landsat TM sensor (Mota et al., 2022). Additionally, improvements in classification algorithms and the availability of higher-quality training data contributed to this enhanced accuracy (Valero-Jorge et al., 2024). Similar findings have been reported by other studies demonstrating the positive impact of improved sensor capabilities and methodological advancements on LULC classification accuracy (Foody, 2020; Sánchez-Llull et al., 2025). The classification accuracy reached its highest level in 2024, achieving an overall accuracy of 93.33% with a Kappa coefficient of 0.88, indicating near-perfect agreement between the classified maps and reference data. This high accuracy is largely due to the superior spatial, spectral, and radiometric resolution of the Landsat OLI sensor, complemented by the application of advanced classification techniques such as machine learning, which effectively handles complex landscapes and mixed pixels (Foody, 2020; Kolić et al., 2025). The progressive improvement in classification accuracy aligns with previous studies demonstrating that enhanced image quality and sophisticated algorithms significantly improve LULC mapping accuracy (Nikolakopoulos & Petropoulos, 2025). The high accuracy achieved in 2024 highlights the reliability of the classification results and strengthens their potential use for analyzing urban change and ecological impacts in Zanzibar.

Change detection analysis

The crosstabulation analysis of 1995 and 2024 land cover maps for urban Zanzibar reveals substantial land cover transitions, with the most prominent change being the conversion of vegetation to built-up areas, amounting to approximately 9,236.88 hectares. This finding indicates extensive urbanization over the nearly three-decade study period, driven by rapid population growth, infrastructure development, and increased economic activities. Similar studies worldwide have reported comparable trends, particularly in developing countries experiencing rapid urban expansion. For instance, a study by Seto et al. (2012) highlights that urban areas in Asia and Africa are expanding at unprecedented rates, resulting in significant loss of vegetation cover and natural habitats. Likewise, Cao et al. (2020) reported substantial conversion of forested and vegetated areas to built-up land in Zhoushan Island, East China due to urban growth, often at the expense of ecological sustainability.

The persistence of built-up areas (1,994.7 ha) underscores the consolidation and stability of urban growth in Zanzibar, reflecting patterns also observed in rapidly urbanizing cities globally. For example, studies conducted in cities across Pacific urban villages have demonstrated similar trends where urban areas continue to expand while remaining relatively stable once established (Jones, 2016). Additionally, the conversion of water to built-up areas



(175.5 ha) highlights coastal development, including the construction of houses, hotels, and other infrastructure, a trend also noted in coastal cities worldwide where tourism-driven urbanization is prevalent (Tew et al., 2018). However, the relatively low transition of built-up areas back to vegetation (499.0 ha) indicates limited urban greening efforts, a phenomenon consistent with findings in cities across Africa and Asia where urbanization is typically associated with irreversible land cover changes (Zhou et al., 2018). Furthermore, the negligible transition from water to vegetation (1.8 ha) likely reflects minor natural processes, such as sediment deposition or vegetation encroachment along water bodies. Collectively, these findings align with broader global patterns of urban expansion and landscape change, underscoring the need for sustainable urban planning to balance development with environmental conservation (Petrisor, et al., 2020).

CONCLUSION

The findings of this study reveal a rapid and extensive urban expansion in Zanzibar from 1995 to 2024, predominantly driven by population growth, infrastructure development, and economic activities. This urbanization has resulted in a significant decline in vegetation cover, with approximately 26.3% of vegetation lost over the study period. Despite the relative stability of water bodies, the conversion of vegetated areas to builtup land highlights the adverse impacts of urban growth on ecological sustainability. The application of advanced remote sensing techniques, including change detection analysis using Landsat imagery, has proven effective in providing a comprehensive understanding of Zanzibar's urbanization patterns. The results emphasize the urgent need for sustainable urban planning and conservation strategies to mitigate the negative environmental consequences of urban sprawl. Future studies should focus on integrating high-resolution satellite data and socio-economic factors to enhance the monitoring and management of urban growth in Zanzibar.

REFERENCES

- Abd El-Hamid, H. T., El-Alfy, M. A., & Elnaggar, A. A. (2020). Prediction of future situation of land use/cover change and modeling sensitivity to pollution in Edku Lake, Egypt based on geospatial analyses. *GeoJournal*.
- African Union. (2021). Agenda 2063: The Africa we want.
- Ahmad, F., Goparaju, L., & Qayum, A. (2017). LULC analysis of urban spaces using Markov chain predictive model at Ranchi in India. *Spatial Information Research*, 25, 351–359.
- Angel, S., Parent, J., & Civco, D. (2021). *Urban expansion* in the world's cities: 2000-2030. Cambridge University Press
- Aziz, F., Kusratmoko, E., & Mandini, M. D. (2020). Estimation of changes in the lake water level and area using remote sensing techniques: Case study: Lake Toba, North Sumatra. *IOP Conference Series: Earth and*

- Environmental Science, 561, 012022.
- Blakime, T. H., Komi, K., Adjonou, K., Hlovor, A. K. D., Gbafa, K. S., Oyedele, P. B., Polorigni, B., & Kokou, K. (2024). Dynamics of built-up areas and challenges of planning and development of urban zone of Greater Lomé in Togo, West Africa. *Land*, 13, 84.
- Cao, W., Li, R., Chi, X., Chen, N., Chen, J., Zhang, H., & Zhang, F. (2017). Island urbanization and its ecological consequences: A case study in the Zhoushan Island, East China. *Ecological Indicators*, 76, 1–14.
- Clarke, K. C. (2018). Cellular automata and agent-based models. In M. Fischer & P. Nijkamp (Eds.), Handbook of regional science. Springer.
- Cohen, J. (1960). A coefficient of agreement for nominal scales. *Educational and Psychological Measurement*, 20(1), 37-46.
- Congalton, R. G. (1991). A review of assessing the accuracy of classifications of remotely sensed data. *Remote Sensing of Environment*, 37(1), 35-46.
- Cottrell, B., Kalacska, M., Arroyo-Mora, J.-P., Lucanus, O., Inamdar, D., Løke, T., & Soffer, R. J. (2024). Limitations of a multispectral UAV sensor for satellite validation and mapping complex vegetation. *Remote Sensing*, 16(13), 2463.
- Eastman, J. R. (2016). TerrSet geospatial monitoring and modeling system manual. Clark Labs, Clark University.
- Jones, P. (2016). The emergence of Pacific urban villages: Urbanization trends in the Pacific Islands.
- Jones, P. (2016). The emergence of Pacific urban villages: Urbanization trends in the Pacific Islands. Asian Development Bank.
- Kolić, J., Pernar, R., Seletković, A., & Ančić, M. (2025). Determining the accuracy of structural parameters measured from LiDAR images in lowland oak forests. *Forests*, 16(2), 340.
- Kukkonen, M., Muhammad, M., Käyhkö, N., & Luoto, M. (2017). Urban expansion in Zanzibar City, Tanzania: Analyzing quantity, spatial patterns, and effects of alternative planning approaches. Land Use Policy, 71.
- Fleiss, J. L., Levin, B., & Paik, M. C. (2003). The measurement of interrater agreement. In W. A. Shewart & S. S. Wilks (Eds.), Statistical methods for rates and proportions (pp. 598–626). John Wiley & Sons Inc.
- Foody, G. M. (2020). Explaining the unsuitability of the kappa coefficient in the assessment and comparison of the accuracy of thematic maps obtained by image classification. *Remote Sensing of Environment*, 239.
- Foody, G. M. (2002). Status of land cover classification accuracy assessment. Remote Sensing of Environment, 80, 185–201.
- Gavade, A. B., & Rajpurohit, V. S. (2020). Sparse-FCM and deep learning for effective classification of land area in multi-spectral satellite images. Evolutionary Intelligence.
- Gidey, E., Dikinya, O., Sebego, R., Segosebe, E., & Zenebe, A. (2017). Cellular automata and Markov Chain (CA_Markov) model-based predictions of future land use and land cover scenarios (2015–2033) in Raya, northern Ethiopia. Modeling Earth Systems and



- Environment, 3, 1245-1262.
- Gokool, S., Mahomed, M., Brewer, K., Naiken, V., Clulow, A., Sibanda, M., & Mabhaudhi, T. (2024). Crop mapping in smallholder farms using unmanned aerial vehicle imagery and geospatial cloud computing infrastructure. *Heliyon*, 10, e26913.
- Günen, M. A., & Atasever, U. H. (2024). Remote sensing and monitoring of water resources: A comparative study of different indices and thresholding methods. *Science of the Total Environment, 926,* 172117.
- Haldar, S., Chatterjee, U., Bhattacharya, S., Paul, S.,
 Bindajam, A. A., Mallick, J., & Abdo, H. G. (2024).
 Peri-urban dynamics: Assessing expansion patterns and influencing factors. *Ecological Processes*, 13, 1.
- Harrak, Y., Rachid, A., & Aguejdad, R. (2025). Evaluation of spectral indices and global thresholding methods for the automatic extraction of built-up areas: An application to a semi-arid climate using Landsat 8 imagery. *Urban Science*, 9(3), 78.
- Huang, Y., Yang, B., Wang, M., Liu, B., & Yang, X. (2020).
 Analysis of the future land cover change in Beijing using CA–Markov chain model. *Environmental Earth Sciences*, 79, 60.
- Jackson, C., & Adam, E. (2021). Machine learning classification of endangered tree species in a tropical submontane forest using WorldView-2 multispectral satellite imagery and imbalanced dataset. Remote Sensing, 13(24).
- Jensen, J. (2005). *Introductory digital image processing: A remote sensing perspective* (4th ed.). Prentice Hall.
- Jia, X., & Richards, J. (1999). Segmented principal components transformation for efficient hyperspectral remote-sensing image display and classification. *IEEE Transactions on Geoscience and Remote Sensing*, 37(1), 25–27.
- Karimi, H., Jafarnezhad, J., Khaledi, J., & Ahmadi, P. (2018). Monitoring and prediction of land use/ land cover changes using CA-Markov model: A case study of Ravansar County in Iran. Arabian Journal of Geosciences, 11, 592.
- Kavzoglu, T., & Mather, P. (2000). Using feature selection techniques to produce smaller neural networks with better generalization capabilities. *Proceedings of the International Geoscience and Remote Sensing Symposium (IGARSS)*, 7, 23–31.
- Lewis, A., Lacey, J., Mecklenburg, S., Ross, J., Siqueira, A., Killough, B., Szantoi, Z., Tadono, T., Rosenqvist, A., Goryl, P., et al. (2018). CEOS analysis-ready data for land (CARD4L) overview. Proceedings of the 2018 IEEE International Geoscience and Remote Sensing Symposium (IGARSS), Valencia, Spain, 7407–7410.
- Li, X., Zhou, Y., Asrar, G. R., & Zhu, Z. (2021). The impacts of urban expansion on climate and environment: A global review. *Environmental Research Letters*, 16(1), 1–20.
- Li, S. H., Jin, B. X., Wei, X. Y., Jiang, Y. Y., & Wang, J. L. (2015). Using CA-Markov model to model the spatiotemporal change of land use/cover in

- Fuxian Lake for decision support. ISPRS Annals of Photogrammetry, Remote Sensing and Spatial Information Sciences, II-4/W2, 163–168.
- Liu, H., Zhang, F., Zhang, L., Lin, Y., Wang, S., & Xie, Y. (2020). UNVI-based time series for vegetation discrimination using separability analysis and random forest classification. Remote Sensing, 12(3), 529.
- Ma, X., Hong, Y., & Song, Y. (2020). Super resolution land cover mapping of hyperspectral images using the deep image prior-based approach. *International Journal* of Remote Sensing, 41, 2818–2834.
- Mishra, S., Shrivastava, P., & Dhurvey, P. (2017). Change detection techniques in remote sensing: A review. International Journal of Wireless and Mobile Communication and Industrial Systems, 4, 1–8.
- Mohamed, M. K., Adam, E., & Jackson, C. M. (2023). Policy review and regulatory challenges and strategies for the sustainable mangrove management in Zanzibar. *Sustainability*, 15, 1557.
- Mohamed, M. K., Adam, E., & Jackson, C. M. (2023). The spatial and temporal distribution of mangrove forest cover from 1973 to 2020 in Chwaka Bay and Menai Bay, Zanzibar. *Applied Sciences*, 13, 7962.
- Mohamed, M. K., Adam, E., & Jackson, C. M. (2024). Assessing the perception and contribution of mangrove ecosystem services to the well-being of coastal communities of Chwaka and Menai Bays, Zanzibar. *Resources*, 13(7).
- Mota, A., Curcino, N., Gioppo, F., Andrade, L., & Assunção, C. F. (2022). Digital image classification: A comparison of classic methods for land cover and land use mapping. *Anuário do Instituto de Geociências*, 45, 1–10.
- Nalepa, J., Myller, M., Imai, Y., Honda, K., Takeda, T., & Antoniak, M. (2019). Unsupervised segmentation of hyperspectral images using 3D convolutional autoencoders. arXiv preprint, arXiv:1907.08870.
- National Bureau of Statistics Tanzania. (2022). 2022 Population and Housing Census: Population distribution by administrative units. National Bureau of Statistics. https://www.nbs.go.tz/uploads/statistics/documents/sw-1720088450-2022%20PHC%20 Initial%20Results%20-%20English.pdf
- Nikolakopoulos, I. A., & Petropoulos, G. P. (2025). Obtaining a land use/cover cartography in a typical Mediterranean agricultural field combining unmanned aerial vehicle data with supervised classifiers. *Land*, 14(3), 643.
- Petrisor, A.-I., Hamma, W., Nguyen, H. D., Randazzo, G., Muzirafuti, A., Stan, M.-I., Tran, V. T., Aşţefănoaiei, R., Bui, Q.-T., Vintilă, D.-F., et al. (2020). Degradation of coastlines under the pressure of urbanization and tourism: Evidence on the change of land systems from Europe, Asia, and Africa. Land, 9, 275.
- Pontius, R. G., & Cheuk, M. L. (2006). A generalized cross-tabulation matrix to compare soft-classified maps at multiple resolutions. *International Journal of Geographical Information Science*, 20(1), 1–30.



- Puplampu, D. A., & Boafo, Y. A. (2021). Exploring the impacts of urban expansion on green spaces availability and delivery of ecosystem services in the Accra Metropolis. *Journal of Environmental Challenges*, 5, 100283.
- Revolutionary Government of Zanzibar. (2019). Zanzibar Strategic Urban Plan: Integrated planning for sustainable development. Ministry of Lands, Housing, Water, and Energy, Zanzibar.
- Revolutionary Government of Zanzibar. (2020). Zanzibar Urban Development Policy: Promoting sustainable urban growth through infrastructure improvement, economic diversification, and environmental resilience. Ministry of Lands, Housing, Water, and Energy, Zanzibar.
- Revolutionary Government of Zanzibar. (2021). Zanzibar Environmental Policy: Enhancing environmental management and resilience. Ministry of Agriculture, Natural Resources, Livestock, and Fisheries, Zanzibar.
- Revolutionary Government of Zanzibar. (2022). Zanzibar Vision 2050: Towards inclusive and sustainable development. President's Office – Finance, Economy, and Development Planning, Zanzibar.
- Roy, D. P., Wulder, M. A., Loveland, T. R., et al. (2014). Landsat-8: Science and product vision for terrestrial global change research. Remote Sensing of Environment, 145, 154–172.
- Sánchez-Llull, M., Castellanos Torres, L., Muñoz Caravaca, A., Martín Morales, G., Sauvage, S., Zulueta-Véliz, Y., Olalde Chang, E. J., León Cabrera, J., Vasallo-Rodríguez, L., Ouillon, S., & Sánchez-Pérez, J.-M. (2025). Assessing classification accuracy as a criterion for evaluating the performance of seven topographic correction algorithms in the Trinidad Mountains, Cuba. *Remote Sensing*, 17(6), 1032.
- Sassen, S. (2021). Cities in a world economy (5th ed.). Sage Publications.
- Satterthwaite, D., Archer, D., & Dodman, D. (2020). Addressing urban inequalities: Policies and implications. *Current Urban Studies*, 8(4), 403–418.
- Seto, K. C., Güneralp, B., & Hutyra, L. R. (2020). Global urban expansion: A multidimensional approach. Annual Review of Environment and Resources, 45, 79–107.
- Seto, K., Reenberg, A., Boone, C., & Fragkias, M. (2012). Urban land teleconnections and sustainability. *Proceedings of the National Academy of Sciences, 109*(29), 13916–13921.
- Shao, Z., Cheng, T., Fu, H., Li, D., & Huang, X. (2023). Emerging issues in mapping urban impervious surfaces using high-resolution remote sensing images. *Remote Sensing*, 15, 2562.
- Tessema, W. M., & Abebe, G. B. (2023). Quantification of land use/land cover dynamics and urban growth in rapidly urbanized countries: The case of Hawassa City, Ethiopia. *Urban Planning and Transport Research*,

- *11*, 1.
- Tew, Y. L., Tan, M. L., Samat, N., & Yang, X. (2019). Urban expansion analysis using Landsat images in Penang, Malaysia. *Sains Malaysiana*, 48(11), 2307–2315.
- Tossoukpe, A. Y., Dukiya, J., Folega, F., Thiel, M., & Okhimamhe, A. A. (2025). Dynamics of changes in spatial patterns of built-up areas in two metropolitan areas of Grand Lomé and Greater Accra (West Africa). *Urban Science*, 9(3), 84.
- Tsurusaki, N., & Salem, M. (2024). Impacts of rapid urban expansion on peri-urban landscapes in the global south: Insights from landscape metrics in Greater Cairo. *Sustainability*, 16, 2316. https://doi.org/10.xxxx/sus16
- UN-Habitat. (2020). The world's cities in 2020: Data booklet. United Nations.
- United Nations. (2019). World urbanization prospects: The 2018 revision. United Nations.
- U.S. Geological Survey. (2021). Landsat collection 2 level-1 and level-2 science products. U.S. Department of the Interior. Retrieved September 23, 2024, from https://www.usgs.gov/landsat-missions/landsat-collection-2
- Vali, A., Comai, S., & Matteucci, M. (2020). Deep learning for land use and land cover classification based on hyperspectral and multispectral Earth observation data: A review. *Remote Sensing*, 12(15), 2495.
- Valero-Jorge, A., González-De Zayas, R., Matos-Pupo, F., Becerra-González, A. L., Álvarez-Taboada, F. (2024). Mapping and monitoring of the invasive species Dichrostachys cinerea (Marabú) in central Cuba using Landsat imagery and machine learning (1994–2022). Remote Sensing, 16, 20.
- World Bank. (2021). Transforming Tanzania's cities: Harnessing urbanization for competitiveness, resilience, and livability. The World Bank.
- Zanotta, D. C., Zortea, M., & Ferreira, M. P. (2018). A supervised approach for simultaneous segmentation and classification of remote sensing images. *ISPRS Journal of Photogrammetry and Remote Sensing*, 142, 162– 173
- Zhang, C., Wang, Q., & Atkinson, P. M. (2025). Unsupervised object-based spectral unmixing for subpixel mapping. Remote Sensing of Environment, 318, 114514.
- Zhou, Y., Li, X., Asrar, G. R., Smith, S. J., & Imhoff, M. (2018). A global record of annual urban dynamics (1992–2013) from nighttime lights. Remote Sensing of Environment, 219, 206–220.
- Wang, M., Cai, L., Xu, H., & Zhao, S. (2019). Predicting land use changes in northern China using logistic regression, cellular automata, and a Markov model. *Arabian Journal of Geosciences*, 12, 790.